*33rd EPS Conference on Plasma Phys. Rome, 19 - 23 June 2006 ECA Vol.**30I**, P-5.155 (2006)*

Improved Computer Simulations of Energy Confinement in the Advanced Reversed-Field Pinch

J.-E. Dahlin, J. Scheffel

Alfvén Laboratory, Royal Institute of Technology, Stockholm, Sweden

A revised algorithm for numerical simulations of the advanced reversed-field pinch (RFP) is presented. The results show more favourable scalings of magnetic fluctuations, energy confinement time τ_E and poloidal beta β_θ with basic initial parameters as compared to what has been presented by the authors in earlier studies of the advanced RFP. In general, enhanced confinement in the advanced RFP stems from the introduction of current profile control (CPC), here implemented through a scheme of active feedback of the electric dynamo field. The work, which has an optimistic approach and sweeps over a large parameter domain, is theoretical and aims to answer the question of how far, *in principle*, CPC can bring the RFP concept towards the reactor domain. Experimental implementation is thus a later concern. With this scheme, a state with strongly suppressed tearing mode activity is achieved, which allows for a theoretical study of pressure driven resistive *g*-modes. This is a task that has been difficult to perform in the past, since tearing modes have always dominated the RFP dynamics. We here present results from two different CPC schemes. Both result in Quasi Single Helicity (QSH) states with high confinement while in the second scheme steady state conditions are approached.

1. Background

Numerical simulations performed in RFP geometry using the resistive MHD computational code DEBSP[1,2], have shown that the scaling of energy confinement time τ_E and poloidal beta β_θ with number density n and total current I is strongly influenced by anomalous transport. The anomalous transport is a result of ergodic magnetic field lines formed in a relaxation process called the RFP dynamo. Indeed, the Lawson parameter $n\tau_E$ does not scale with the basic parameters towards reactor conditions in the conventional RFP[3,4].

The dynamo process is a redistribution process of poloidal current throughout the minor radius, and is a result of resistive tearing mode activity. The dynamo fluctuations can be described by the theory of plasma diffusion and relaxation[5,6]. Although the RFP is a strongly shear stabilized configuration, it is brought to an unstable state through resistive diffusion, being driven by the plasma current gradient. Energy and particles are transported towards the outer plasma as the magnetic field lines become ergodic through tearing mode activity. The configuration reassumes a minimum energy state by a self-organisation process on the Alfvén time scale, and the periodic behaviour starts over again. In this process, the fluctuating (dynamo) electric field $E_f = - \langle v \times B \rangle$ drives the required poloidal current for relaxation (brackets indicate mean value over poloidal and toroidal directions).

In this study a series of resistive magnetohydrodynamic numerical simulations are performed to generate scaling laws for energy confinement time τ_E and poloidal beta β_θ for the advanced RFP. Strongly increased confinement is obtained for the advanced RFP as compared to the conventional RFP, which stems from the introduction of CPC.

Many schemes for CPC have been suggested[7-10], both for numerical and experimental applications. In order to perform a large number of simulations to establish a data base for scaling laws for the confinement parameters, it is crucial to minimize the number of free numerical parameters. In the numerical simulations, CPC is performed by implementation of a *parameter free* automatic feedback algorithm, optimized to reduce the fluctuation caused electric field. The scheme introduces an ad-hoc electric field within the plasma volume, automatically adjusted to dynamically control the plasma into more quiescent behaviour by eliminating current driven tearing mode instabilities and reducing resistive interchange modes.

2. Numerical simulations

The CPC scheme used in this study[11] determines the parallel component of the dynamo field, E_f, and replaces it with an ad hoc parallel electric auxiliary field E_a:

$$E_a(t) = -k_I \int_0^t E_f(t)dt \approx -k_I \sum E_f(t)\Delta t \quad (1)$$

The numerical simulation tool is the resistive MHD code DEBSP. The auxiliary field is introduced into the momentum equation (neglecting viscosity) as:

$$\rho \frac{dv}{dt} = j \times B - \nabla p + F_a \quad (2)$$

and in Ohm's law as:

$$E = -\langle v \times B \rangle + \eta j - E_a \quad (3)$$

where the force term F_a is related to the electric field E_a as $F_a = -neE_a$, in SI units.

3. Results I

As seen in figure 1, the energy confinement time τ_E and the poloidal beta β_θ increases and the radial magnetic field component (squared and averaged) $\langle B_r^2 \rangle$ decreases substantially as the CPC is switched on (approximately at time t = 0.0125 τ_R). Figure 2 shows that the dynamo field E_f decreases by two orders of magnitude – even more in the core region where it is almost completely eliminated. However, some irreducible activity persists in the edge region. It is unclear exactly what mechanism might be responsible for the persisting edge activity. A likely candidate is resistive *g*-modes that cannot be stabilized completely by the CPC due to unfavourable curvature and negative pressure gradient.

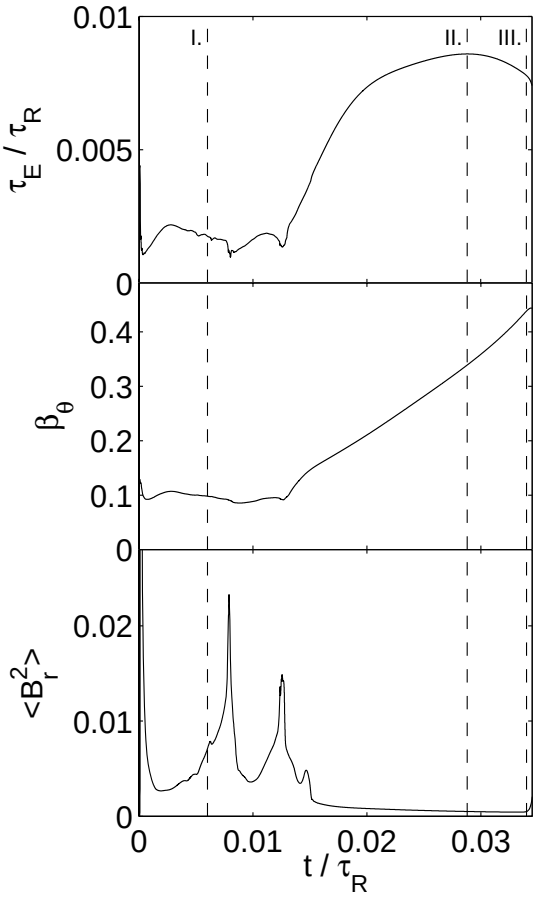

Figure 1. Energy confinement time τ_E, poloidal beta β_θ and radial magnetic field (squared and averaged) $\langle B_r^2 \rangle$ as functions of (resistive) time. Vertical dashed bars indicate times t_1, t_2 and t_3.

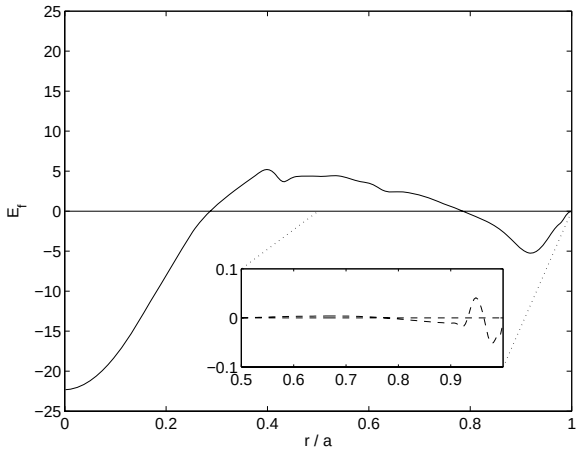

Figure 2. Radial profile for the fluctuating dynamo field $|E_f|$ for time t_1 (general view) and time t_2 (magnified view).

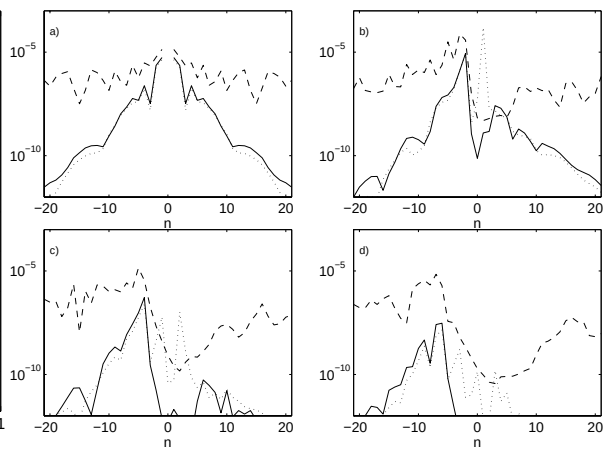

Figure 3. Mode spectra for a) m = 0, b) m = 1, c) m = 2 and d) m = 3 and n-modes through -21 to 21. Negative n indicate modes internal to the reversal surface while positive n indicate external modes. Dashed lines indicate modes at time t_1, solid lines at time t_2 and dotted lines at time t_3.

The mode spectra (figure 3) give much information on what mechanisms are in effect both during the enhanced confinement period and later during the eventual decrease in energy confinement. At time t_2 (see figure 1 for an indication of time numbers), i.e. during the enhanced confinement period, all modes are principally suppressed. The dominant mode at time t_2 is the (m, n) = (1,-2) mode, which is resonant in the core plasma. The configuration has developed into a Quasi Single Helicity (QSH) state where the plasma dynamics is dictated by one dominant mode and only slightly affected by secondary modes. Such a state may be beneficial from the energy confinement point of view.

As the configuration continues to evolve from the QSH state into an unstable state where the energy confinement time eventually drops, one other mode rises and dominates at time t_3. This mode is (m, n) = (1, 1), and it becomes resonant at the plasma edge when the q-profile drops towards q = -1 close to the wall due to the very strong field reversal. The appearance of this mode is possibly the reason for the decrease of energy confinement. However, it is difficult to conclude whether this mode is current driven or pressure driven since driving forces for both mechanism exist at the plasma edge.

In a previous paper, scaling laws were presented for confinement parameters, based on a series of computer simulations for a set of initial parameter values:

$$\beta_p = 0.246\Theta^{0.23} a^{-0.058} \mu^{0.029} Z_{eff}^{0.058} \left(I/N\right)^{-0.12} I^{-0.12} \tag{4}$$

$$T(0) = 8.6\cdot 10^{8} \Theta^{-1.5} a^{-0.13} \mu^{0.064} Z_{eff}^{0.13} \left(I/N\right)^{0.74} I^{0.74} \tag{5}$$

$$\tau_E = 196\Theta^{-1.0} a^{1.5} \mu^{0.25} Z_{eff}^{-0.50} \left(I/N\right)^{0.50} I^{0.50} \tag{6}$$

4. Results II

The fact that a steady state is not achieved for the CPC scheme described, and that the energy confinement time peaks, is a problem from the view of establishing a reactor relevant system of enhanced energy confinement. The chain of events seems to be the following: The feedback routine tries to eliminate the persisting activity in the E_f-field in

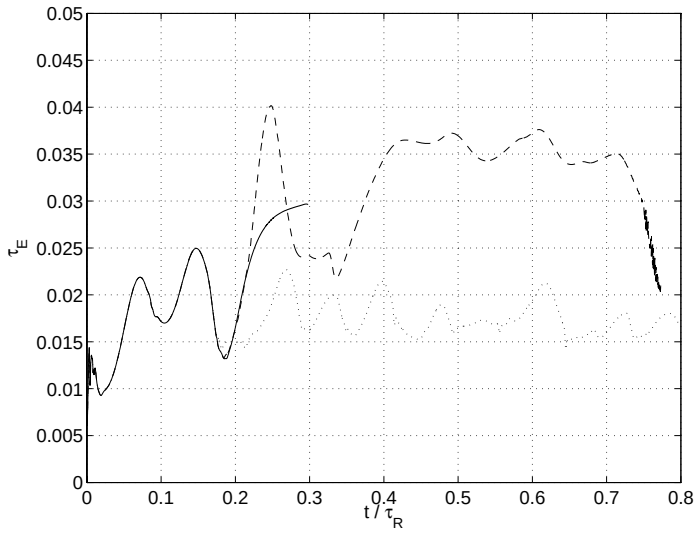

Figure 4. Energy confinement time τ_E for various cases. Dotted line is a reference case without CPC, solid line is the first CPC scheme and dashed line is the second CPC scheme.

the edge region, which obviously is not possible. Thus the field reversal becomes even stronger and the q-value becomes very high in the core plasma meanwhile approaching -1 at the plasma edge. The (m, n) = (1, 1) mode is triggered and energy confinement decreases. A cure for the runaway effect would thus be to not compensate for a certain allowable residual E_f-field.

In our second CPC scheme, the parameter $|E_f^{tol}|$ is introduced. As long as $|E_f| > |E_f^{tol}|$ the CPC feedback is switched on, but as $|E_f| \leq |E_f^{tol}|$ it is switched off, and the ad hoc auxiliary field E_a is made to decrease gradually. Eventually $|E_f|$ becomes a little larger than $|E_f^{tol}|$ and the process starts over again. The fluctuations are seen in time traces of the energy confinement time. In figure 4 three cases are shown: a reference case without CPC, the case with the previously described CPC and the case employing the second CPC scheme. Indeed a steady state is achieved for the later, and the energy confinement time is higher than for the first scheme. The final decrease in energy confinement time appears to be caused by a numerical instability.

5. Conclusions and discussion

It is found that RFP confinement increases substantially when active feedback CPC is employed. Two different scenarios are studied, both attaining a QSH state. The first scheme is constrained by a runaway effect, for which the dynamics is carefully studied, but for the second scheme a quasi steady state is achieved.

This work is theoretical and it remains to be determined whether the results can be reproduced experimentally. However, the objective has been to investigate the theoretical potential for active CPC.

References

1. D. D. Schnack and D. C. Baxter, J. Comput. Phys. 55, 485 (1984).
2. D. D. Schnack et. al., Comput. Phys. Commun. 43, 17 (1986).
3. J. Scheffel and D. D. Schnack, Phys. Rev. Lett. 85, 322 (2000).
4. J. Scheffel and D. D. Schnack, Nucl. Fusion 40, 1885 (2000).
5. J. B. Taylor, Phys. Rev. Lett. 33, 1139 (1974).
6. D. D. Schnack and S. Ortolani, in *Magnetohydrodynamics of Plasma Relaxation*, (Singapore, 1993).
7. J. S. Sarff et. al., Phys. Rev. Lett. 72, 3670 (1994).
8. M. R. Stoneking et. al., Phys. Plasmas 4, 1632 (1997).
9. J. S. Sarff, N. E. Lanier, S. C. Prager, and M. R. Stoneking, Phys. Rev. Lett. 78, 62 (1997).
10. C. R. Sovinec and S. C. Prager, Nucl. Fusion 39, 777 (1999).
11. J.-E. Dahlin and J. Scheffel, Phys. Plasmas 12, 062502 (2005).